Piezoresistive Polymer Diaphragm Sensor Array Using Conductive Elastomeric Nanocomposite Films for Skin-Mountable Keypad Applications

Jeong-Ho Kong, Nam-Su Jang, Jin-Yeop Huh, Soo-Hyung Kim, and Jong-Man Kim

***Abstract*— This paper reports on arrayed piezoresistive polymer diaphragm sensor made entirely of elastomer for skin-mountable keypad applications. Two-step transfer of conductive elastomeric nanocomposites (CENs) combined with soft lithographic techniques enables the achievement of elastic sensing layers with strip-patterned CENs embedded in polydimethylsiloxane (PDMS) channels. After assembling with an elastomeric bump layer, simple all-elastomer sensor architectures are successfully demonstrated. The activated buttons of the sensor can be easily and distinguishably identified by sensing the simultaneous changes in the electrical resistance of CEN strips with respect to the applied force. The straightforward sensing mechanism makes it possible to detect the exact locations of input with negligible crosstalk between adjacent sensing buttons to each other. The usability of the sensor platform as a skin-mountable keypad is also demonstrated by integrating on a wrist. [2014-0072]**

***Index Terms*— Piezoresistive polymer diaphragm sensor, conductive elastomeric nanocomposites, skin-mountable keypad.**

I. Introduction

PIEZORESISTIVE transducers that can induce changes in electrical resistance in response to deformations have been widely employed in various sensor applications due to their compact structure and simple sensing and readout mechanism. So far, various types of piezoresistive materials, architectures, and fabrication methodologies have been extensively studied to develop a broad range of compact sensing platforms, including pressure sensors and tactile sensors [1]–[26]. In the early stage, thin rigid diaphragms integrated with piezoresistors were most widely used as piezoresistive sensor platforms with the advances in three-dimensional microfabrication technologies [7]–[14]. Although they show high sensitivity and good spatial resolution, achieving mechanical robustness of the devices under sudden impact or large deformation is challenging mainly due to the fragility of the thin diaphragms. In addition, multi-step processes are inevitably required for the fabrication of sensing elements, electrical interconnects, and supporting diaphragms, resulting in complex and expensive fabrication. Most critically, conventional diaphragm-based piezoresistive sensors were generally fabricated on rigid silicon substrates, and are thus not suitable for being applied to curved or complex surfaces as an array-configured architecture.

For skin-mountable applications, several methods have recently been developed to demonstrate piezoresistive sensor arrays in flexible or stretchable forms [15]–[26]. Flexible tactile sensor arrays were prepared by a substrate release technique [15]–[17]. In this approach, sensor arrays are first fabricated on a rigid substrate coated with photo-patternable polymers based on standard microfabrication techniques, and become flexible by releasing the polymer layer from the carrier substrate after fabrication. This approach is quite systematic, but still suffers from complex and expensive fabrication due to the multi-step processing. Carbon fibers (CFs) aligned individually on an elastomeric substrate were used as arrayed piezoresistors to detect normal force [18]. However, this method may be not suitable for mass-production due to the complexity of micro-manipulation of the CFs. Piezoresistive strain sensors based on ultrathin single-crystalline silicon (SCS) ribbons printed on flexible substrates were developed [19]. Although the devices showed high gauge factor of $\sim$43 under uniaxial tensile strain by using SCS with superior piezoresistive effects, they may be of limited application due to the low strain limits

A new class of piezoresistor array based on conductive liquid-filled elastomeric micro-channels was used for wearable tactile keypad applications [20]. The unique sensor structures can facilitate conformal contact even with complex surfaces due to their extreme flexibility. Nevertheless, a critical drawback includes a possible leakage of the conductive liquid after multiple uses, which may hinder long-term stability. More recently, some have reported that conductive nanoplatforms such as conductive sponges [21], conductive filler-embedded polymer nanocomposites [22], [23], and vertically aligned carbon nanotubes [24] can be employed as pressure-sensitive films. In spite of their simple configurations, signal crosstalk among adjacent sensing elements may be a big challenge, because the piezoresistive materials are formed as continuous film geometries in their system. Alternatively, piezoresistive nanocomposites were site-selectively dispensed onto a flexible substrate with data transmission wires [25], [26]. Although this

Manuscript received March 5, 2014; revised June 13, 2014; accepted July 8, 2014. Date of publication July 29, 2014; date of current version June 1, 2015. This research was supported by the Civil and Military Technology Cooperation Program through the National Research Foundation of Korea (NRF) funded by Ministry of Science, ICT and Future Planning (No. 2013M3C1A9055407). This work was also supported by the Industry-University Co-Innovation Project, Republic of Korea. Subject Editor E.-S. Kim.

J.-H. Kong and N.-S. Jang are with the Department of Nano Fusion Technology, Pusan National University, Busan 609-735, Korea (e-mail: whilewhale@pusan.ac.kr; jns1016@naver.com).

J.-Y. Huh, S.-H. Kim, and J.-M. Kim are with the Department of Nanomechatronics Engineering, Pusan National University, Busan 609-735, Korea (e-mail: mopea102@nate.com; sookim@pusan.ac.kr; jongkim@pusan.ac.kr).

Color versions of one or more of the figures in this paper are available online at http://ieeexplore.ieee.org.

Digital Object Identifier 10.1109/JMEMS.2014.2338332

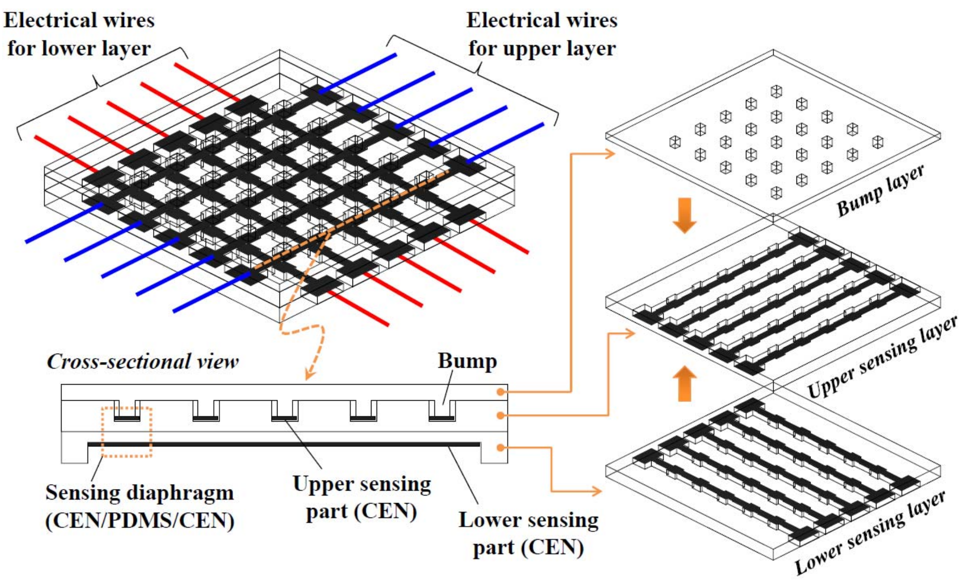

Fig. 1. Perspective view of 5 × 5 piezoresistive polymer diaphragm sensor arrays.

approach can reduce the signal crosstalk by isolating sensing elements from each other, the whole fabrication would be quite cumbersome and time-consuming.

In the present work, we report an all-elastomer platformed keypad with 25 independent buttons that can detect exact pressing locations without appreciable crosstalk. Each piezoresistive button embedded in the sensor is composed of an elastic diaphragm incorporated with conductive elastomeric nanocomposite (CEN) films employed as piezoresistors. A combination of soft lithography and two-step transfer of CENs enables the fabrication to be simple and potentially scalable. All-elastomer sensor architectures are mechanically robust against various elastic deformations and highly suitable for being integrated on the curved or complex surfaces of human body parts.

II. Design and Fabrication

A. Sensor Architecture and Working Principle

Fig. 1 shows a schematic illustration of the 5 × 5 piezoresistive polymer diaphragm sensor arrays proposed in this work. The all-elastomer sensor platform (30 × 30 mm^2) consists of upper and lower PDMS layers with strip-patterned CEN films for sensing a normal force and subsequently tracing the change in the electrical properties of the films with respect to the applied force. The piezoresistive polymer diaphragms (1.08 × 1.08 mm^2) made of a PDMS layer sandwiched in between the CEN films are constructed by assembling the two sensing layers with the CEN strips embedded in PDMS channels while aligning perpendicular to each other, as shown in Fig. 1. This facile strategy makes it possible to achieve simple diaphragm architectures that can be employed as piezoresistive transducers without additional structures for mechanically supporting the diaphragms. A top PDMS layer with flat-top bumps higher than the depth of the PDMS channels is used to raise the physical deformation of the sensing parts in response to the normal force. Top area of the bumps in contact with sensing diaphragms was designed to 860 × 860 μm^2, which is smaller than that of the diaphragms, for easy integration with the sensing layer.

The sensing principle of the proposed sensor array is illustrated schematically in Fig. 2. When a normal force is applied to the sensing diaphragm through the PDMS bump, the maximum stress occurs at the regions in contact with the bump edges. Several contact junctions among the multiwalled carbon nanotubes (MWCNTs) in the PDMS matrix are lost or weakened due to local stretching of the CEN films at the stress-concentrated regions, resulting in loss of some current paths (red arrows in Fig. 2) and subsequent increase in the electrical resistance [27], [28]. In principle, the structural deformation of the sensing diaphragms in response to the applied normal force induces changes in the electrical resistance of both the upper and lower CEN films at the same time, as shown in Fig. 2. Therefore, the pressed points can be easily recognized by tracing the simultaneous resistance changes in the two sensing layers.

B. Fabrication Details

In the proposed sensor architectures, CEN films play a great role in both detecting external normal force by the intrinsic piezoresistivity and ensuring mechanical robustness. Prior to micropatterning, the CENs were synthesized by simply doping MWCNTs into PDMS matrix as in the following procedures: (1) MWCNTs (7 wt%) were first mixed in a volatile toluene solution at a weight ratio of 1:10 by sonicating for 1 hr, followed by stirring magnetically for 2 hr to improve the dispersion of the MWCNTs. In this case, the concentration of the MWCNTs was carefully optimized. One can easily expect that lower filler concentration is more desirable for obtaining higher sensitivity of the devices. This would originate from the fact that current paths in the MWCNT electrcial networks at a low concentration can be more easily lost under deformation, compared to densely entangled networks (high concentration). At a concentration of less than 7 wt%, however, the electrical

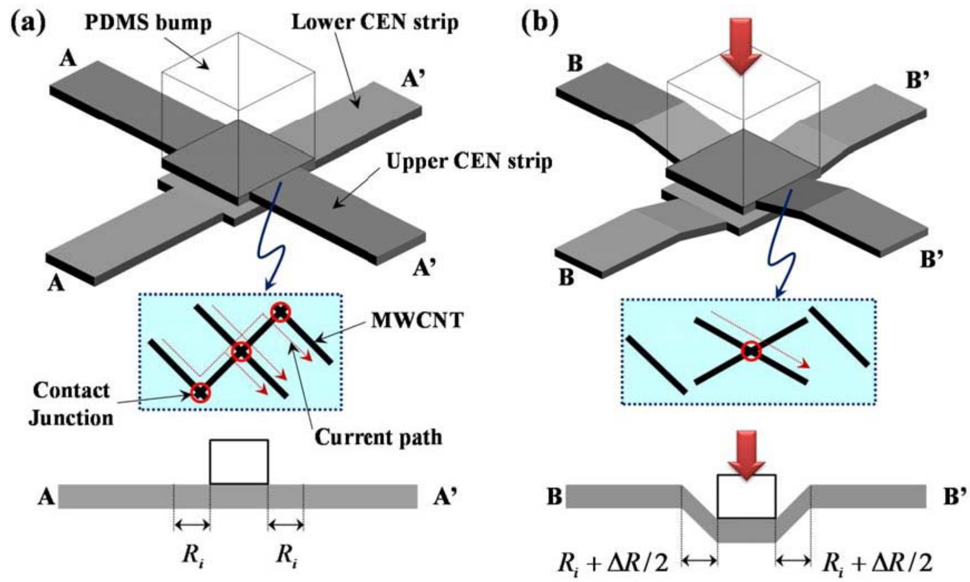

Fig. 2. Schematic illustrations of sensing principle of the proposed sensor platform. (a) initial state and (b) activated state.

conductivity of the CENs was quite unstable, which can hinder stable operations of the sensors. In addition, high viscosity of the CENs with increasing MWCNT concentrations (>7 wt%) made it difficult to produce CEN patterns based on the contact printing approach. Therefore, the optimal concentration of the MWCNTs was designed to 7 wt% with considerations of both high sensitivity and good processability. (2) The MWCNT suspension was then added to PDMS prepolymer (Sylgard 184 A, Dow Corning) diluted with the toluene solution at a weight ratio of 1:1. (3) The MWCNT/PDMS/toluene mixture was stirred magnetically on an 80 °C hotplate while entirely evaporating the solvent components in the mixture. (4) Finally, the CENs were prepared by mixing the PDMS prepolymer doped with 7 wt% MWCNTs and a curing agent (Sylgard 184 A, Dow Corning).

The proposed piezoresistive polymer diaphragm sensor array is fabricated by a simple combination of soft lithography and two-step transfer of CENs. A detailed fabrication process of the sensor array is illustrated schematically in Fig. 3. For the fabrication of sensing layers, ~80-μm-thick photoresist (PR, JSR-THB-151N) patterns, which are employed both as stamps and replica molds, were first defined photolithographically on a four-inch silicon substrate (Fig. 3(a-1)). The CENs that were squeezed on another silicon substrate were then transferred selectively onto the protruding parts of the prepared polymer stamp by a facile contact printing technique using a manual z-axis stage (Fig. 3(a-2)).

Prior to the use of CENs, the nanocomposites were degassed in a desiccator equipped with a vacuum pump for 1 hr to fully remove air bubbles inside. Next, PDMS prepolymer mixed with a curing agent at 10:1 weight ratio was poured onto the stamp substrate printed with CENs, followed by curing thermally at 70 °C for 30 min in a convection oven (Fig. 3(a-3)). When peeling off the polymerized PDMS from the stamp, the CEN strip patterns on the stamp were entirely transferred into the PDMS channels (Fig. 3(a-4)). This is probably facilitated by the fact that uncured CENs and PDMS prepolymer can be homogeneously binded after curing, which also promotes mechanical robustness of the sensor platform by preventing any delamination of the CEN strips under various deformations. The upper and lower sensing layers were prepared by the same procedures described above.

For the fabrication of the bump layer, ~100-μm-thick polymer replica molds were formed on a four-inch silicon wafer using a standard photolithographic process. PDMS prepolymer with a curing agent (10:1) was poured onto the replica molds with square holes and subsequently cured thermally at 70 °C for 30 min (Fig. 3(b-1)). After peeling off from the mold substrate, the PDMS bump layer was prepared (Fig. 3(b-2)).

The all-elastomer sensor architectures were fabricated by assembling the prepared PDMS sensing (upper and lower) and bump layers. Prior to assembly, all the PDMS surfaces on the bonding sides were pre-treated by exposure to oxygen (O_2) plasma to allow for strong bonding interfaces by making them hydrophilic and reactive. The fabricated PDMS bump layer was first bonded to the prepared sensing layer after aligning carefully. Next, another PDMS sensing layer was then assembled with the bonded bump-sensing layer while perpendicularly aligning the CEN strips in the upper and lower sensing layers to each other (Fig. 3(c-1)). The fabrication of the sensor platform was completed by connecting electrical wires for measurements on the exposed probing electrodes using a silver paste (Fig. 3(c-2)).

III. Results and Discussion

A. Fabrication Results

Fig. 4(a) shows a digital image of the piezoresistive polymer diaphragm sensor array laid on a paper with the logo of our institution, which indicates that the transparent PDMS windows between the CEN strips enable the patterns underlying the sensor platform to be distinguished.

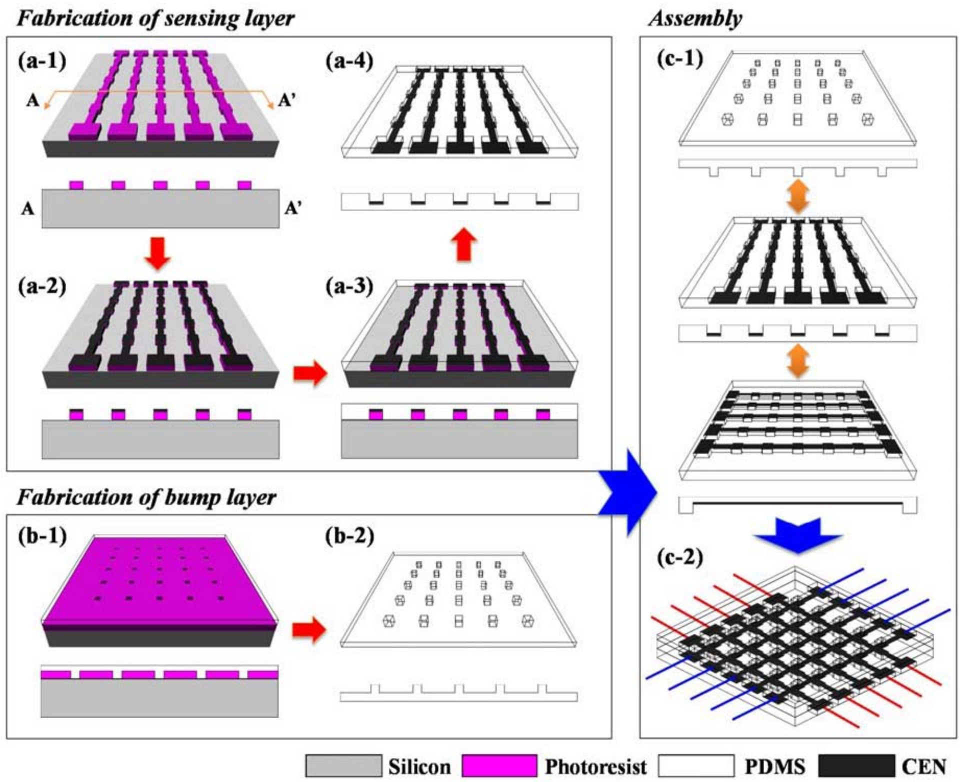

Fig. 3. Schematic illustrations of fabrication process of the proposed sensor platform. (a) sensing layers: (a-1) PR pattern formation for stamps and replica molds, (a-2) contact transfer of CENs, (a-3) PDMS pouring and subsequent curing, (a-4) replication of sensing layers, (b) bump layer: (b-1) replica mold formation and PDMS pouring/curing, (b-2) replication of bump layer, and (c) assembly: (c-1) align bonding of sensing and bump layers after O_2 plasma treatment, (c-2) electrical wiring.

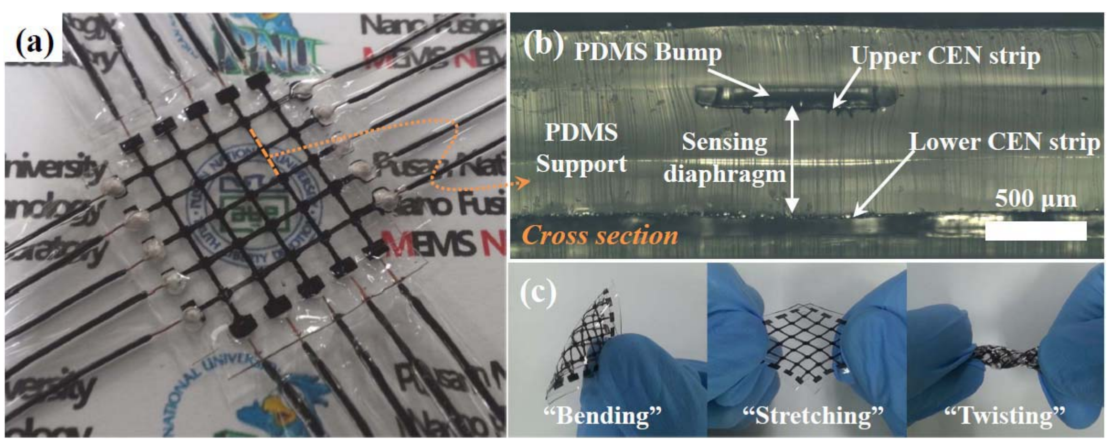

Fig. 4. Fabrication results of the sensing platform. (a) digital image of the fabricated sensor array, (b) cross-sectional optical microscopy image of the sensor platform, and (c) digital images of the fabricated all-elastomer sensor platform under bending, stretching, and twisting deformations.

The fabricated sensor architecture was observed more precisely with cross-sectional profiles prepared using an optical microscope (BX60M, OLYMPUS) equipped with a CCD module, as shown in Fig. 4(b). The thickness of the fabricated sensor platform was as thin as ~1 mm. It was clearly seen that the piezoresistive diaphragm (~530 μm in thickness) sandwiched with the CEN films is incorporated stably with the homogeneous PDMS supports, and all the PDMS layers are well established without any appreciable interfacial defects such as voids or exfoliation. In addition, the structural robustness of the device against various mechanical deformations such as bending, stretching, and twisting was clearly demonstrated based on its all-elastomer architecture, as shown in Fig. 4(c).

B. Sensing Performance

The sensing performance of the fabricated device was evaluated by measuring the resistance change ratio ($\Delta R/R_0$)

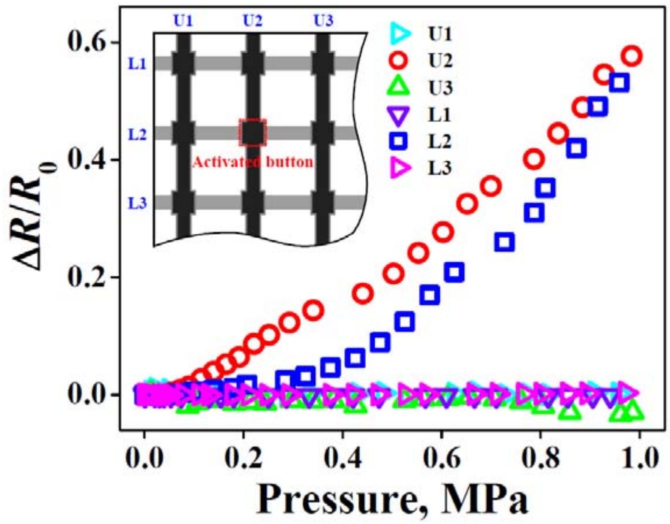

Fig. 5. Resistance change ratios measured on the CEN strips when the pressure of up to 1 MPa to a sensing diaphragm at (2, 2).

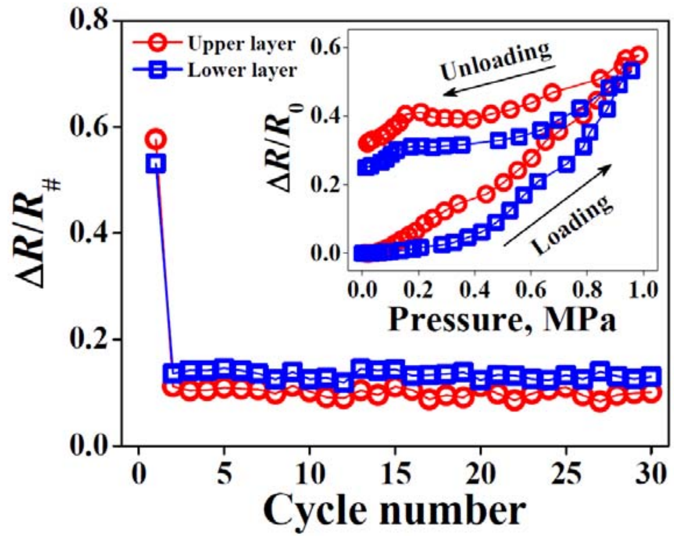

Fig. 6. Resistance changes of CEN strips in a sensing button at (2, 2) under repetitive tests of up to 30 cycles with a maximum pressure of 1 MPa (inset: $\Delta R/R_0$ of CEN strips at first pressure loading and unloading).

of the upper and lower CEN strips as a function of pressure. For this, normal force was applied to a target piezoresistive diaphragm by a flat-top cylindrical tip (diameter: ∼5 mm) using an automatic testing stand (JSV-H1000, JISC) equipped with a digital push-pull force gauge (HF-10, JISC) at a constant loading speed of 1 mm/min. The electrical resistances of the upper and lower CEN strips in response to the applied force were simultaneously measured and recorded in real time using two digital multimeters (U1253B, Agilent Technologies) interfaced independently to a computer with RS-232 data cables.

Fig. 5 shows the $\Delta R/R_0$ measured on the CEN strips when pressure of up to 1 MPa was applied to a sensing diaphragm at (2, 2), which indicates the overlapped point of the second upper (U2) and the second lower (L2) CEN strips, as illustrated in the inset figure. The initical electrical resistances of U2 and L2 on the as-prepared sensor platform were measured to 11.5 kΩ and 11.7 kΩ, respectively. With the application of pressure, the electrical resistances of U2 and L2 were simultaneously increased due to the loss of several current paths at the stress-concentrated regions in the CEN films. The gradual increase of the resistance suggests that more current paths were lost with increasing pressure. On the other hand, the electrical properties of CEN strips (U1, U3, L1, and L3) adjacent to the pressurized sensing cell were retained without considerable changes under the same pressure, as shown in Fig. 5. This clearly suggests that the sensing cell at (2, 2) can be recognized as an activated button among the 25 buttons in the device without the influence of crosstalk. This would originate from the fact that the electrical resistane of the CEN strips physically isolated from each other is independently changed due to the local stretching at the stress-concentrated regions in each CEN strip.

Fig. 6 shows the resistance changes ($\Delta R/R_{\#}$) of the CEN strips consisting of the diaphragm at (2, 2) under repetitive pressure loadings and subsequent unloadings of up to 30 cycles with a maximum pressure of 1 MPa. Here, $R_{\#}$ indicates the initial resistance of each cycle. In general, nanofiller-doped conductive nanocomposites show hysteretic behavior under deformation, which means that the electrical properties that were changed by the applied force are not perfectly recovered to the initial states, even when the force is fully removed [29]–[33]. Although the hysteretic behaviors were also found on the fabricated CEN strips in the first cycle (inset of Fig. 6), the sensor responses became stable after a few cycles, as shown in Fig. 6. This originates from the fact that the electrical resistances in the initial and pressed states were fairly stabilized without significant deviation after the preconditioning phase. In particular, the resistances in the initial and pressed states of the upper layer were 12.7 ± 0.19 kΩ and 14 ± 0.22 kΩ for the last 20 cycles, respectively. For the lower layer, the initial resistance of 12.2 ± 0.19 kΩ was changed to 13.8 ± 0.24 kΩ after pressing. This is probably due to the fact that MWCNT networks in as-prepared CEN films are rearranged while being geometrically stabilized during the early cycles. In this stabilization period, several contact junctions in the MWCNT networks might experience irreversible deformations, leading to a rise of an intrinsic resistance of CEN strips. Although this degrades the piezoresistivity of CEN strips upon pressing, the stabilized sensor responses should be greatly desirable for their practical use.

In addition, the electrical robustness of the sensor platform under various mechanical deformations, such as bending, stretching and twisting, was examined by monitoring the resistance changes of a pair of CEN strips in response to the deformations. Fig. 7 shows the resistance changes of the CEN strips (U4 and L4) under the mechanical deformations. Relatively slow recovery characteristics were found probably due to the viscoelastic property of PDMS. Nevertheless, the electrical resistances of the CEN strips in each deformed state almost returned to those in their initial states when releasing the loads, indicating good reversibility. This suggests that the device is quite reliable even under various types of

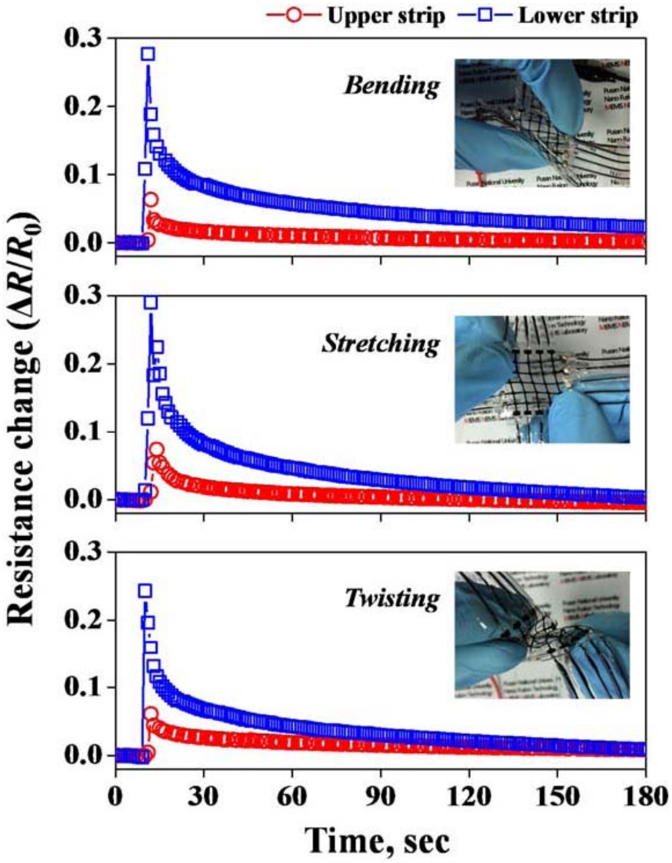

Fig. 7. Resistance change ratios of the CEN strips (U4 and L4) under bending, stretching and twisting deformations.

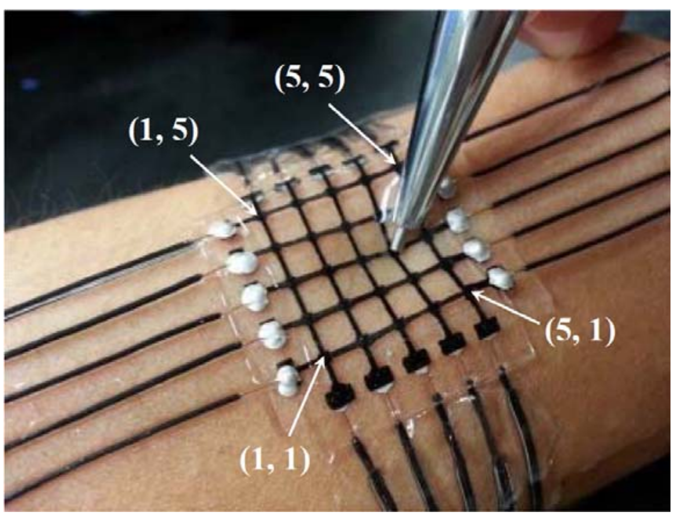

Fig. 8. Digital image of the all-elastomer sensor array integrated on a wrist.

deformations thanks to the mechanically stable all-elastomer architectures.

C. Practical Demonstration

The usability of the piezoresistive polymer diaphragm sensor array as a skin-mountable keypad was demonstrated by integrating the fabricated device on a wrist, as shown in Fig. 8.

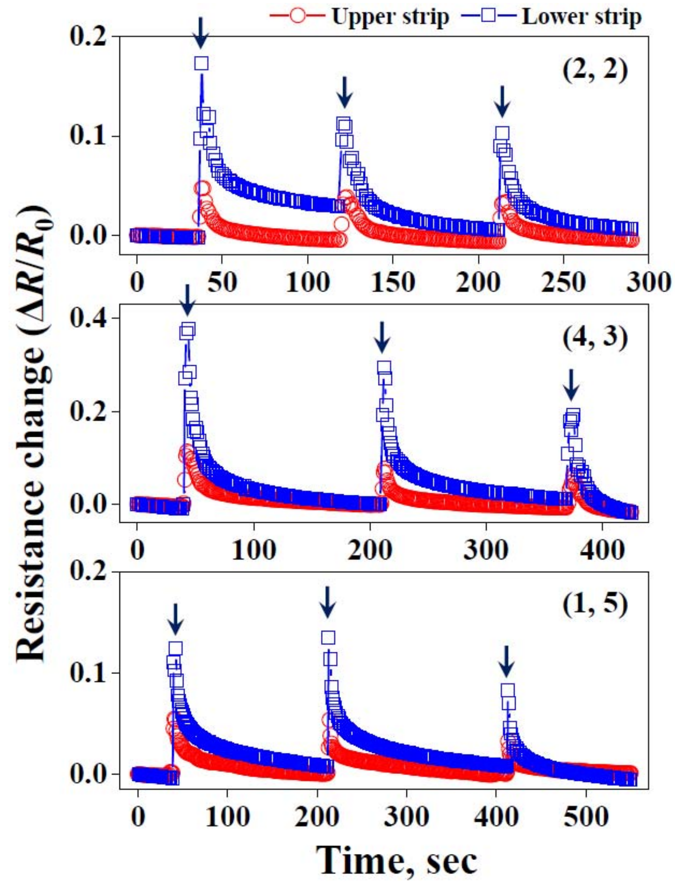

Fig. 9. Resistance change ratios of the CEN strips in 3 randomly selected buttons of the sensor platform integrated on the wrist under the application of pressure three times in succession.

The input pressure was applied to target buttons manually using a sharp pencil by hand. Fig. 9 shows the resistance changes of the CEN strips in 3 randomly selected buttons (at (2, 2), (4, 3), and (1, 5)) of the sensor platform integrated on the wrist under the application of pressure three times in succession. The arrows in Fig. 9 indicate the moment when activating buttons. The tested buttons responded immediately to the applied force without appreciable time delay. Although the recovery was also relatively slow, the experimental observation clearly suggests that the proposed skin-mountable sensor platform can sufficiently and distinguishably detect the hitting events.

IV. Conclusion

In summary, a skin-mountable keypad sensor platform with piezoresistive polymer diaphragm buttons that can clearly and distinguishably detect hitting events has been presented. A combination of soft lithography and two-step transfer of conductive elastomeric nanocomposites (CEN) films enabled the fabrication to be simple and potentially scalable. In addition, all-elastomer architectures are greatly desirable for achieving mechanical robustness with respect to various deformations and mounting easily and conformally, even on complex surfaces. Finally, the integration of the sensor platform on a wrist clearly demonstrated the possibility of its use in practical skin-mountable applications.

References

[1] A. D. Smith *et al.*, "Electromechanical piezoresistive sensing in suspended graphene membranes," *Nano Lett.*, vol. 13, no. 7, pp. 3237–3242, Jul. 2013.

[2] N. Thanh-Vinh, N. Binh-Khiem, H. Takahashi, K. Matsumoto, and I. Shimoyama, "High-sensitivity triaxial tactile sensor with elastic microstructures pressing on piezoresistive cantilevers," *Sens. Actuators A, Phys.*, vol. 215, pp. 167–175, Aug. 2014.

[3] A. Wisitsoraat, V. Patthanasetakul, T. Lomas, and A. Tuantranont, "Low cost thin film based piezoresistive MEMS tactile sensor," *Sens. Actuators A, Phys.*, vol. 139, nos. 1–2, pp. 17–22, Sep. 2007.

[4] K. Noda, K. Hoshino, K. Matsumoto, and I. Shimoyama, "A shear stress sensor for tactile sensing with the piezoresistive cantilever standing in elastic material," *Sens. Actuators A, Phys.*, vol. 127, no. 2, pp. 295–301, Mar. 2006.

[5] H. Takahashi, A. Nakai, N. Thanh-Vinh, K. Matsumoto, and I. Shimoyama, "A triaxial tactile sensor without crosstalk using pairs of piezoresistive beams with sidewall doping," *Sens. Actuators A, Phys.*, vol. 199, no. 1, pp. 43–48, Sep. 2013.

[6] D. Alvares, L. Wieczorek, B. Raguse, F. Ladouceur, and N. H. Lovell, "An evaluation study of nanoparticle films as biomimetic tactile sensors," *Sens. Actuators A, Phys.*, vol. 186, pp. 148–153, Oct. 2012.

[7] Y. Matsuoka *et al.*, "Low-pressure measurement limits for silicon piezoresistive circular diaphragm sensors," *J. Micromech. Microeng.*, vol. 5, no. 1, pp. 32–35, Mar. 1995.

[8] W. P. Eaton and J. H. Smith, "Micromachined pressure sensors: Review and recent developments," *Smart Mater. Struct.*, vol. 6, no. 5, pp. 530–539, Oct. 1997.

[9] B. J. Kane, M. R. Cutkosky, and G. T. A. Kovacs, "A traction stress sensor array for use in high-resolution robotic tactile imaging," *J. Microelectromech. Syst.*, vol. 9, no. 4, pp. 425–434, Dec. 2000.

[10] M. Shikida, T. Shimizu, K. Sato, and K. Itoigawa, "Active tactile sensor for detecting contact force and hardness of an object," *Sens. Actuators A, Phys.*, vol. 103, no. 1, pp. 213–218, Jan. 2003.

[11] A. Berns, U. Buder, E. Obermeier, A. Wolter, and A. Leder, "AeroMEMS sensor array for high-resolution wall pressure measurements," *Sens. Actuators A, Phys.*, vol. 132, no. 1, pp. 104–111, Nov. 2006.

[12] A. Tibrewala, A. Phataralaoha, and S. Büttgenbach, "Simulation, fabrication and characterization of a 3D piezoresistive force sensor," *Sens. Actuators A, Phys.*, vol. 147, no. 2, pp. 430–435, Oct. 2008.

[13] M. P. Orthner, S. Buetefisch, J. Magda, L. W. Rieth, and F. Solzbacher, "Development, fabrication, and characterization of hydrogel based piezoresistive pressure sensors with perforated diaphragms," *Sens. Actuators A, Phys.*, vol. 161, nos. 1–2, pp. 29–38, Jun. 2010.

[14] Y. Xu, "Post-CMOS and post-MEMS compatible flexible skin technologies: A review," *IEEE Sensors J.*, vol. 13, no. 10, pp. 3962–3975, Oct. 2013.

[15] J. Engel, J. Chen, and C. Liu, "Development of polyimide flexible tactile sensor skin," *J. Micromech. Microeng.*, vol. 13, no. 3, pp. 359–366, May 2003.

[16] J.-C. Lee and D.-W. Lee, "Flexible and tactile sensor based on a photosensitive polymer," *Microelectron. Eng.*, vol. 87, nos. 5–8, pp. 1400–1403, May/Aug. 2010.

[17] K. Kim *et al.*, "Polymer-based flexible tactile sensor up to 32 × 32 arrays integrated with interconnection terminals," *Sens. Actuators A, Phys.*, vol. 156, no. 2, pp. 284–291, Dec. 2009.

[18] C.-S. Park, J. Park, and D.-W. Lee, "A piezoresistive tactile sensor based on carbon fibers and polymer substrates," *Microelectron. Eng.*, vol. 86, nos. 4–6, pp. 1250–1253, Apr./Jun. 2009.

[19] S. M. Won *et al.*, "Piezoresistive strain sensors and multiplexed arrays using assemblies of single-crystalline silicon nanoribbons on plastic substrates," *IEEE Trans. Electron Devices*, vol. 58, no. 11, pp. 4074–4078, Nov. 2011.

[20] R. K. Kramer, C. Majidi, and R. J. Wood, "Wearable tactile keypad with stretchable artificial skin," in *Proc. IEEE Int. Conf. Robot. Autom.*, May 2011, pp. 1103–1107.

[21] H.-B. Yao *et al.*, "A flexible and highly pressure-sensitive graphene–polyurethane sponge based on fractured microstructure design," *Adv. Mater.*, vol. 25, no. 46, pp. 6692–6698, Dec. 2013.

[22] H. Wang, D. Zhou, and J. Cao, "Development of a skin-like tactile sensor array for curved surface," *IEEE Sensors J.*, vol. 14, no. 1, pp. 55–61, Jan. 2014.

[23] G. Canavese, S. Stassi, M. Stralla, C. Bignardi, and C. F. Pirri, "Stretchable and conformable metal–polymer piezoresistive hybrid system," *Sens. Actuators A, Phys.*, vol. 186, pp. 191–197, Oct. 2012.

[24] O. Yilmazoglu *et al.*, "Vertically aligned multiwalled carbon nanotubes for pressure, tactile and vibration sensing," *Nanotechnology*, vol. 23, no. 8, p. 085501, Mar. 2012.

[25] M.-Y. Cheng, C.-M. Tsao, Y.-Z. Lai, and Y.-J. Yang, "The development of a highly twistable tactile sensing array with stretchable helical electrodes," *Sens. Actuators A, Phys.*, vol. 166, no. 2, pp. 226–233, Apr. 2011.

[26] Y.-J. Yang *et al.*, "An integrated flexible temperature and tactile sensing array using PI-copper films," *Sens. Actuators A, Phys.*, vol. 143, no. 1, pp. 143–153, May 2008.

[27] W. Xu and M. G. Allen, "Deformable strain sensors based on patterned MWCNTs/polydimethylsiloxane composites," *J. Polym. Sci., Part B, Polym. Phys.*, vol. 51, no. 20, pp. 1505–1512, Oct. 2013.

[28] C.-X. Liu and J.-W. Choi, "Strain-dependent resistance of PDMS and carbon nanotubes composite microstructures," *IEEE Trans. Nanotechnol.*, vol. 9, no. 5, pp. 590–595, Sep. 2010.

[29] M. Knite, V. Tupureina, A. Fuith, J. Zavickis, and V. Teteris, "Polyisoprene-multi-wall carbon nanotube composites for sensing strain," *Mater. Sci. Eng. C, Mater. Biol. Appl.*, vol. 27, nos. 5–8, pp. 1125–1128, Sep. 2007.

[30] E. T. Thostenson and T.-W. Chou, "Real-time in situ sensing of damage evolution in advanced fiber composites using carbon nanotube networks," *Nanotechnology*, vol. 19, no. 21, p. 215713, May 2008.

[31] Y. Zhang *et al.*, "Polymer-embedded carbon nanotube ribbons for stretchable conductors," *Adv. Mater.*, vol. 22, no. 28, pp. 3027–3031, Jul. 2010.

[32] L. Lin, S. Liu, S. Fu, S. Zhang, H. Deng, and Q. Fu, "Fabrication of highly stretchable conductors via morphological control of carbon nanotube network," *Small*, vol. 9, no. 21, pp. 3620–3626, Nov. 2013.

[33] M. K. Shin, J. Oh, M. Lima, M. E. Kozlov, S. J. Kim, and R. H. Baughman, "Elastomeric conductive composites based on carbon nanotube forests," *Adv. Mater.*, vol. 22, no. 24, pp. 2663–2667, Jun. 2010.

Jeong-Ho Kong received the M.S. degree in nanofusion technology from Pusan National University, Busan, Korea, in 2014. He is currently an Assistant Engineer with Samsung Electronics Company, Ltd., Suwon, Korea.

His current research interests include flexible/stretchable electronics based on conductive nanocomposites, human-motion sensing, and nano/micro manufacturing processes and systems.

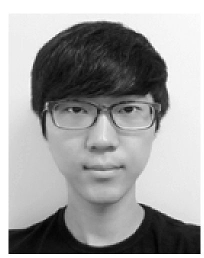

Nam-Su Jang received the M.S. degree in nanofusion technology from Pusan National University, Busan, Korea, in 2014, where he is currently pursuing the Ph.D. degree.

His current research interests include synthesis and applications of functional nanomaterials, micromachined sensors and actuators, and flexible/stretchable devices.

Jin-Yeop Huh is currently pursuing the B.S. degree in nanomechatronics engineering with Pusan National University, Busan, Korea.

His current research interests include synthesis of conductive nanocomposites, polymer-based nano/micro machining technologies, and skin-mountable elastic sensor platforms.

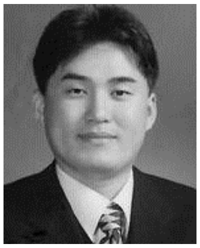

Soo-Hyung Kim received the Ph.D. degree in mechanical engineering from the University of Minnesota, Minneapolis, MN, USA, in 2003. In 2006, he joined Pusan National University, Busan, Korea, where he is currently an Associate Professor of Nanomechatronics Engineering (undergraduate) and Nano Fusion Technology (graduate).

His current research interests include synthesis and characterization of nanostructured materials, and their applications to the fields of photovoltaic and electronic devices.

Jong-Man Kim received the Ph.D. degree in electrical engineering and computer science from Seoul National University, Seoul, Korea, in 2007. In 2008, he joined Pusan National University, Busan, Korea, where he is currently an Associate Professor of Nanomechatronics Engineering (undergraduate) and Nano Fusion Technology (graduate).

His current research interests include design, fabrication, and characterization of MEMS sensors and actuators, biomimetic engineering, synthesis and applications of functional nanomaterials, and flexible/stretchable electronics.